www.czasopisma.pan.pl PAN POLSKA AKADEMIA NAUK www.journals.pan.pl

Arch. Metall. Mater. **67** (2022), 2, 735-742

DOI: https://doi.org/10.24425/amm.2022.137812

M. HOJNY[1*], T. DĘBIŃSKI[1]

A NOVEL FE/MC-BASED MATHEMATICAL MODEL OF MUSHY STEEL DEFORMATION WITH GPU SUPPORT

The paper presents the results of work leading to the construction of a spatial hybrid model based on finite element (FE) and Monte Carlo (MC) methods allowing the computer simulation of physical phenomena accompanying the steel sample testing at temperatures that are characteristic for soft-reduction process. The proposed solution includes local density variations at the level of mechanical solution (the incompressibility condition was replaced with the condition of mass conservation), and at the same time simulates the grain growth in a comprehensive resistance heating process combined with a local remelting followed by free/controlled cooling of the sample tested. Simulation of grain growth in the entire computing domain would not be possible without the support of GPU processors. There was a 59-fold increase in the computing speed on the GPU compared to single-threaded computing on the CPU. The study was complemented by examples of experimental and computer simulation results, showing the correctness of the adopted model assumptions.

Keywords: FEM; Monte Carlo; extra-high temperatures; soft-reduction; GPU

1. Introduction

Physical and computer simulation research on integrated processes is now one of priority trends in the development of innovative manufacturing processes of steel products [1]. These processes feature combining continuous casting and rolling processes into a single production line. The process of integrated steel strip casting and rolling can be an example of such solution [2]. The soft reduction process is the final stage of the continuous casting technology, wherein a semi-solid strand is deformed with casting machine rolls. Accordingly, from the model point of view, it is a variety of the rolling process. Problems related to the final product quality often occur in actual industrial processes. The occurring temperature ranges with a reduced plasticity have a significant impact on the quality of the strand cast and rolled. If a critical process stage is within the cast steel reduced plasticity range, there is a high likelihood of crack initiation in the strand cast. Therefore, it is necessary to know the occurrence of temperature ranges with a lower plasticity and high-temperature mechanical properties, to be able to control the actual industrial process so as to minimize the occurrence of cracks in the strand cast. The formulated mathematical model should be fully spatial, despite the fact that the mechanical state that occurs during the strand deformation in lower temperature ranges can be deemed flat. In temperature ranges close to the solidus line, two zones can be distinguished in the volume of the strand deformed: the solid zone and the mushy zone with a complex geometry. The comprehensive model for the soft-reduction and integrated casting and rolling processes can be shared, as long as the material behavior both in the solid and in the semi-solid state is taken into account. It is strictly related to the use of appropriate constitutive equations determining the characteristics of plastic flow of the strand deformed. The main reason for limitation of the numerical modeling of deformation in the semi-solid state is the fact that most mechanical and physical properties of the material tested are unknown. The emergence of Gleeble thermo-mechanical simulators in the market has caused a rapid increase in research possibilities as regards research on steel deformation in extra-high temperatures, primarily in the semi-solid state [3]. These simulators are basically the only devices available in the market, allowing extra-high temperature tests to be conducted. As the development of continuous steel casting and rolling techniques in recent years has been very intensive, research in this field with the use of the aforementioned thermo-mechanical simulators now constitutes the basic research foundation for the development of new techniques [4,5]. The increasing availability of modern

[1] AGH UNIVERSITY OF SCIENCE AND TECHNOLOGY, AL. MICKIEWICZA 30, 30-059 KRAKOW, POLAND,

* Corresponding author: mhojny@agh.edu.pl

instruments (3D scanning systems, computer tomography), and most of all thermo-mechanical simulators has resulted in the beginning of research and scientific work on steel deformation in temperature ranges near the solidus line [6-11]. Research on the steel deformation in the semi-solid state, carried out by the authors of papers and many other researchers, constitutes a research foundation for modeling and designing innovative new integrated casting and rolling techniques, including the soft-reduction process. At the same time, from the engineering point of view, there is continuous striving to simplify or eliminate some operations, which eventually would significantly reduce energy costs. On the other hand, it is better for the natural environment (less industrial waste or reduced emissions of noxious gases and dusts). Accordingly, most of the studies have a common conclusion that controlled casting and rolling of strands is necessary. Therefore, results of numerical and physical simulations of the process examined will be useful to control the process parameters. Analyzing the available specialized literature [6-11], we can observe a gap as there are no comprehensive solutions concerning broadly understood modeling of steel deformation in the semi-solid state. This concerns primarily the area of experimental tests themselves, and the development of new mathematical models. The mathematical model presented in this paper bridges the gap in this research area. The solution is original as it includes local density variations in the mechanical model at the level of mechanical solution, and a simultaneous simulation of grain growth in a comprehensive resistance heating process combined with a local remelting followed by the free/controlled cooling of the sample tested in the tool system of a Gleeble 3800 thermo-mechanical simulator. Additionally, GPU support was used in order to increase the computational efficiency of the grain growth model. The use of CUDA architecture [12] allowed for effective calculations of grain growth in the entire computational domain.

2. Experimental methodology

Experimental tests were performed using a Gleeble 3800 thermo-mechanical simulator and a Hydrawedge unit [14]. The research was divided into two main stages. During the first stage, a cycle of tensile/compression tests was performed to identify coefficients of the rheological model of the steel S355 tested. The objective of the second stage was to provide data for initial verification of the formulated hybrid model. Cylindrical samples Ø10×124 mm (Fig. 1A) and cuboidal samples with a cross-section 10×10 mm and a length of 124 mm were used (Fig. 1B). In all variants, both ends of the samples were fixed in copper grips cooled with water.

The tests were conducted in vacuum with a small addition of argon. The experiment plan was proposed on the basis of the determined solidus T_s and liquidus T_l temperatures of the steel tested (1465°C and 1513°C, respectively). The samples were heated to the temperature of 1400°C at a rate of 20°C/s. Within the temperature range 1400°C-1450°C slow heating at a rate of 1°C/s was applied, followed by holding for 10-30 seconds at a temperature of 1450°C to stabilize the temperature within the sample volume. Next, controlled cooling at a rate of 10°C/s to the nominal deformation temperature was performed. Samples were deformed by compression or tension at a stroke rate 1 and 20 mm/s and a stroke of 5 mm (compression test). Tensile tests were performed until the sample failure. During the experiments, the

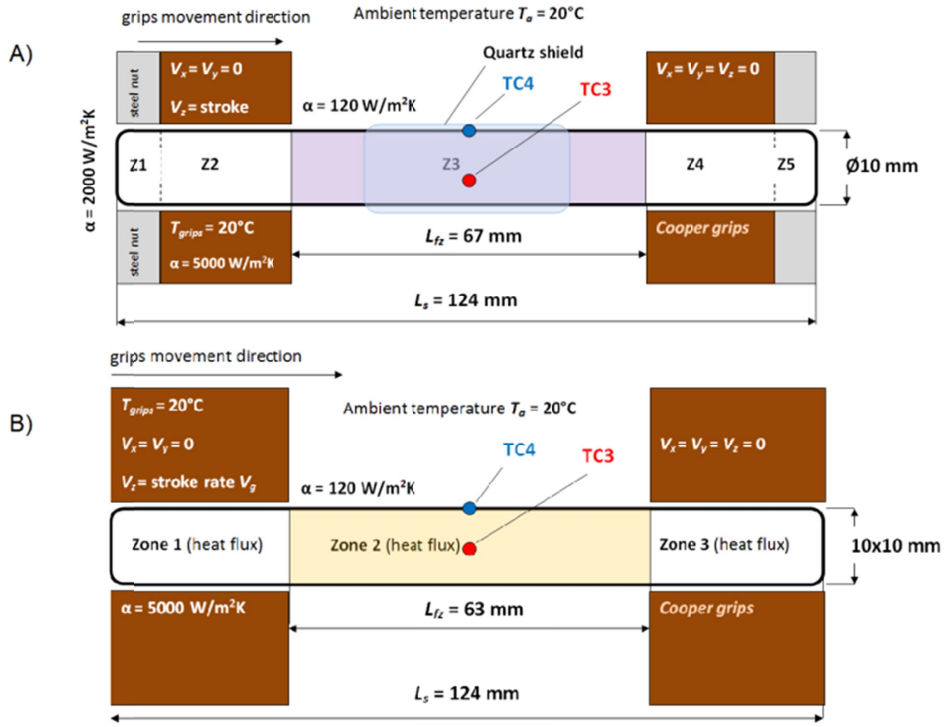

Fig. 1. Sample geometry, boundary conditions, initial conditions and the arrangement of thermocouples, A) the first stage of tests, B) the second stage of tests

following parameters were measured: characteristics of changes in current intensity versus time, force versus tool stroke and temperature at the sample surface (thermocouple TC4, Fig. 1) and the sample core temperature (thermocouple TC3, Fig. 1). After the completed experiment, the samples were scanned in 3D with a 3D ATOS Triple Scan photogrammetric system. Then, using the 3D scanner firmware, the deformed zone length and the deformation zone cross-section dimensions were measured. The final stage of work involved macro-structural examinations of the selected samples to estimate the range of occurrence of zones with diverse dynamics of grain growth.

3. Mathematical model

3.1. Mechanical model

The formulated mathematical model is a hybrid solution combining the finite element (FE) with the Monte Carlo (MC) method. The finite element method is the foundation of the thermo-mechanical solution for the macro scale as regards the simulation of resistance heating combined with local remelting of the sample, followed by its deformation. The strain field and deviatoric stress were determined with a modified rigid-plastic model of a continuum. The classic rigid-plastic solution was modified by substituting the non-compressibility condition (conservation of volume) with the controlled compressibility condition (condition of mass conservation), which is described by the operator equation [13,14]:

$$\nabla\bar{v} - \frac{1}{\rho}\frac{\partial\rho}{\partial\tau} \tag{1}$$

and the functional J of the rigid-plastic solution assumes the following form:

$$J\left[\bar{v}\right] = \int_{\Omega}\sigma_p\dot{\varepsilon}_i d\Omega + \int_{\Omega}\lambda\left(\nabla\bar{v} - \frac{1}{\rho}\frac{\partial\rho}{\partial\tau}\right)d\Omega \tag{2}$$

where: $\bar{v} = (v_x, v_y, v_z)$ – vector velocity field, ρ – density, τ – time, σ_p – yield stress, $\dot{\varepsilon}_i$ – strain rate intensity, Ω – volume of the medium concerned, λ – penalty coefficient. The hydrostatic stress components were determined on the basis of two coupled solutions. The rigid-plastic solution using the Levy-Mises law, which can be written as:

$$s_{ij} = \frac{2}{3}\frac{\sigma_p}{\dot{\varepsilon}_i}\dot{\varepsilon}_{ij} \tag{3}$$

where: s_{ij} – deviatoric stress components, $\dot{\varepsilon}_{ij}$ – strain tensor components, and the numerical solution of the Navier equations, which for a spatial coordinate system assume the form [13]:

$$\begin{aligned}
\frac{\partial\sigma_{xx}}{\partial x} + \frac{\partial\sigma_{yx}}{\partial y} + \frac{\partial\sigma_{zx}}{\partial z} &= 0\\
\frac{\partial\sigma_{xy}}{\partial x} + \frac{\partial\sigma_{yy}}{\partial y} + \frac{\partial\sigma_{zy}}{\partial z} &= 0\\
\frac{\partial\sigma_{xz}}{\partial x} + \frac{\partial\sigma_{yz}}{\partial y} + \frac{\partial\sigma_{zz}}{\partial z} &= 0
\end{aligned} \tag{4}$$

The solution leads to the following form of a differential equation [13]:

$$\frac{\partial\sigma_m(x,y,z)}{\partial x} + \frac{\partial\sigma_m(x,y,z)}{\partial y} + \frac{\partial\sigma_m(x,y,z)}{\partial z} = f(x,y,z) \tag{5}$$

where: $\sigma_{ij} = \sigma_{ji}$ – stress tensor components, σ_m – hydrostatic stress components.

The function $f(x,y,z)$ occurring in equation (5) depends on the yield stress, strain intensity, components of the strain rate tensor and derivatives with respect to x,y,z. These parameters were determined on the basis of the velocity field obtained as a result of optimization of the power functional (2), assuming the known form of the curve describing changes of the yield stress. The function $f(x,y,z)$ present in equation (5), should be deemed known for the presented formulation. Thus the only unknown in equation (5) is the stress distribution function $\sigma_m = \sigma_m(x,y,z)$. The solution to differential equation (5) for the set boundary conditions and known components of the strain tensor allows us to determine the distribution of hydrostatic stress components σ_m. Adding the components of this tensor to the respective components of the deviatoric stress, obtained from the rigid-plastic solution, allows us to determine the complete stress tensor. In the solution presented, changes of stress versus strain ε, stroke rate $\dot{\varepsilon}$, temperature T and liquid phase fraction f_l were taken into account, by adopting the following equation $\sigma_p = f(\varepsilon,\dot{\varepsilon},T,f_l)$:

$$\sigma_p = \frac{\varepsilon^n}{\alpha}ASINH\left[\left(\frac{\dot{\varepsilon}}{A}\right)^m \exp\left(\frac{mQ}{RT}\right)\right](1-\beta f_l) \tag{6}$$

where: R – gas constant [8.314 J/molK]. The coefficients α,β,m,n,Q,A present in equation (6) were identified on the basis of the Direct Identification Methodology, wherein stress-strain curves obtained directly from the experiment were optimized, and the Numerical Identification Methodology, wherein the searched coefficients of equation (6) were established using inverse computing [14]. In studies aiming at developing a rheological model of the steel tested, the following objective functions were defined for optimizing procedures, for the DIM and NIM respectively [14]:

$$F_{DIM}(x) = \frac{1}{N}\frac{1}{N_{mp}}\sum_{i=1}^{N}\sum_{j=1}^{N_{mp}}\left[\frac{\sigma^c_{n,ij} - \sigma^e_{n,ij}}{\sigma^e_{n,ij}}\right]^2 \tag{7}$$

$$F_{NIM}(x) = \frac{1}{N}\frac{1}{N_{mp}}\sum_{i=1}^{N}\sum_{j=1}^{N_{mp}}\left[\frac{F^c_{n,ij} - F^e_{n,ij}}{F^e_{n,ij}}\right]^2 \tag{8}$$

In equations (7) and (8), N, N_{mp} are the numbers of compression/tensile tests and measurement points (stress/force), respectively, σ^e_n, σ^c_n is the nominal stress obtained by the experiment and simulation, and F^e_n, F^c_n are forces from the experiment and numerical simulation, respectively. Calculations aiming at identification of coefficients of vector x in equations (7) and (8) were conducted using gradient-free methods [14].

3.2. Thermal model

The temperature field for a transient heat flow without convection was determined by solving the Fourier-Kirchhoff equation, which in the form without heat convection can be written as [13,14]:

$$k\left(\frac{\partial^2 T}{\partial x^2}+\frac{\partial^2 T}{\partial y^2}+\frac{\partial^2 T}{\partial z^2}\right)+\left(Q-\rho c_p\frac{\partial T}{\partial \tau}\right) \tag{9}$$

where: k – thermal conductivity, Q – heat generation rate, c_p – specific heat. The solution of equation (10) requires correctly determined boundary and initial conditions. The boundary conditions were adapted in accordance with the experiment conducted within the Gleeble 3800 thermo-mechanical simulator tool system (see Fig. 1). The initial condition was the known distribution of temperature within the sample volume, which was 20°C. The heat discharge to the environment and copper grips was modeled in each of the zones Z_s, where s is the number of the subsequent heat transfer zone (see Fig. 1), in the form of defined heat fluxes q_s:

$$q_s=\alpha_z(T-T_0) \tag{10}$$

where: α_z – substitute heat transfer coefficient, T_0 – ambient/tool temperature. A constant value of the substitute heat transfer coefficient of 5000 W/m^{2}K was assumed within the area of tool and sample contact. For the zones wherein heat transfer to the environment occurred, the value of substitute heat transfer coefficient was 120 W/m^{2}K. Heating of tools was not included in the simulations. The tool temperature and the ambient temperature of 20°C were assumed as the initial condition. The heat generated as a result of resistance heating was modeled on the assumption that in the model it would correspond to voluminal heat sources, with powers proportional to the square of electric current intensity I, resistance R and the intensity function H, whose characteristic was identified on the basis of experimental data [14]:

$$Q=H(\tau)\left[I^2(\tau)R(T)\right] \tag{11}$$

The solidification heat in the numerical model was modeled using the enthalpy approach with approximation of thermal capacity (substitute capacity) [14]. The thermo-physical properties in the function of temperature, such as density, specific heat, latent heat, enthalpy, electrical resistivity and thermal conductivity, were computed using the computing module of JMatPro (on the basis of the chemical composition of the steel S355 tested).

3.3. Grain-growth model

The implemented Monte Carlo algorithm is based on minimization of the system energy, wherein local energy changes E are computed using the Hamiltonian:

$$E=J\sum_{(i_m,j_m)}\left(1-\delta_{i_m j_m}\right) \tag{12}$$

where: J – grain boundary energy, δ – Kronecker delta, i_m,j_m – cell and neighbor number. The general algorithm of the coupled solution of MCFE is executed as follows: 1) a simulation of heating/remelting/cooling to determine the temperature field distribution within the sample volume (FE model), 2) an interpolation of node temperatures of the finite element mesh of the macro model onto the micro model cells (for the set integration steps), 3) a random selection of cells and an attempt to change their state (identifier Q_{grain} defining belonging to a specific grain orientation), 4) a change of the state is accepted with a probability:

$$P=B_m(T)e^{-\frac{\Delta E}{kT}}\quad \Delta E>0 \tag{13}$$

$$P=B_m(T)\,\Delta E\le 0 \tag{14}$$

where: P – probability function, kT – modeling parameter, ΔE – change of energy. In equations (14) and (15) $B_m(T)$ a boundary mobility function exists, taking into account impact of diverse values of temperature in individual areas of sample volume on the probability value. In the computing, the following form of the boundary mobility function was assumed [14,15]:

$$B_m(T)=\frac{(T-20)^n}{(T_l-20)^n} \tag{15}$$

where: n – exponent of mobility function. Simulation of remelting and cooling is conducted as follows: 1) if the temperature of the sampled cell is higher than the solidus temperature T_s, the cell state is changed to a random state different than the states of its neighbors (remelting stage), 2) if the temperature of the sampled cell decreases, the classic growth algorithm is executed (cooling stage). The correlation between the simulation time and the number of MC method steps was obtained by applying a linear dependence between these values.

4. Mathematical model verification – example results

4.1. Modeling of high-temperature mechanical properties

One of the fundamental dependences describing plastic behavior of the deformed medium at extremely high temperatures (as well as close to the solidus line) is the dependence of the stress value on strain, strain rate, temperature, and liquid phase fraction [14]. The rheological model of steel S355 selected for the tests was divided into four temperature ranges: 20-700°C, 700-1200°C, 1200-1425°C and over 1425°C. In the temperature range up to 1425°C, the Direct Identification Methodology [14] was applied, which optimizes experimental data obtained directly from tensile tests for the selected nominal temperatures and the tool stroke rate (Gleeble 3800 thermo-mechanical simulator). In this methodology, it was assumed that nominal strain ε_n was the quotient of elongation ΔL (the stroke of the moving tool in the simulator system) and effective working zone L_0, nominal strain rate $\dot{\varepsilon}_n$ was the quotient of tool stroke rate $stroke_{rate}$ and

TABLE 1

Direct Identification Methodology – summary of the obtained coefficients

T, (°C)	α, (MPa^{-1})	n	A, (s^{-1})	m	Q, (J/mol)	e_{mean}
20-700	0.0018747647	0.3988701	1.25E+17	0.010061946	329831.4	12.17
700-1200	0.098361924	0.3494103	1.15E+17	1.065561	464576.7	14.37
1200-1425	0.054623641	0.2089816	1.65E+17	0.1855337	511111.2	11.91

TABLE 2

Numerical Identification Methodology – summary of the obtained coefficients

T, (°C)	α, (MPa^{-1})	n	A, (s^{-1})	m	Q, (J/mol)	β	e_{mean}
>1425	0.0185348	0.1609031	1.33E+17	0.1901114	386152.1	1.07413	14.30

effective working zone L_0, and nominal stress σ_{nom} was the quotient of tensile force F_t and initial cross-sectional area S_0. The estimated value L_0 of 20 mm and the nominal temperature T_n equal to the sample surface temperature (reading of the control thermocouple TC4 in individual tensile tests, see Fig. 1) was assumed in the computing. The coefficients occurring in equation (6) were identified by adopting the aforesaid assumptions, the defined objective function (7) using gradient-free methods [14]. TABLE 1 summarizes coefficients obtained as a result of DIM application. To evaluate the discrepancy between predictions and measurements, the following mean error was used:

$$e_{mean} = F^{1/2} \tag{16}$$

where F is the cost function (Equation 7 and 8).

In the temperature range above 1425°C, the coefficients of equation (6) were identified on the basis of the Numerical Identification Methodology based on inverse computing [14]. The simulation of the direct problem was conducted using the numerical model presented in section 3. Inverse computing was performed on the basis of the objective function (8), by minimizing the difference between the values of measured and computed forces (compression tests). The liquid fraction share for individual Gauss integration points was determined with the analytical Scheil equation [14], on the basis of node temperatures obtained as a result of direct solution for individual time steps. The identified coefficients of equation (6) resulting from inverse computing are summarized in TABLE 2.

TABLE 3 and 4 summarize the computed and measured maximum values of forces in the conducted tests/simulations of tension and compression. The maximum relative error (error between maximum forces recorder during experiments and predictions) was 28.5% for a tensile test at a nominal temperature of 1200°C. In other cases, the relative error oscillated within the range 3.4-9.1%.

TABLE 3

Summary of measured and computed maximum values of forces in tensile and compression tests (stroke rate 1 mm/s)

Stroke rate 1 mm/s	**Tension**			**Compression**
Nominal temperature (°C)	1200	1300	1350	1425
Experiment (N)	1738	1422	1196	1528
Simulation (N)	2233	1551	1291	1644
Relative error (%)	**28.5**	**9.1**	**7.9**	**7.6**

TABLE 4

Summary of measured and computed maximum values of forces in tensile and compression tests (stroke rate 20 mm/s)

Stroke rate 20 mm/s	**Tension**			**Compression**
Nominal temperature (°C)	1200	1300	1350	1425
Experiment (N)	3143	2058	1845	2456
Simulation (N)	2857	1978	1703	2539
Relative error (%)	**9.1**	**3.89**	**7.69**	**3.4**

On the basis of the obtained preliminary results one can find that the formulated rheological model of the steel tested combined with the thermo-mechanical model with a variable density (see section 3) allows us to correctly predict tendencies of changes in force parameters of the high-temperature deformation process.

4.2. Modeling of the resistance heating and grain growth – example results

The resistance heating of samples in the tool system of a Gleeble 3800 thermo-mechanical simulator leads to the obtaining of a heterogeneous temperature field within the sample volume [14,15]. In the analyzed temperature range close to the solidus line, even small local temperature changes cause rapid changes in mechanical properties [14,16]. This directly affects the accuracy of predicting force parameters such as the size and shape of the deformation zone obtained. Fig. 2 present the calculated temperature fields for the selected stages of heating to a nominal temperature of 1435°C. Analyzing the obtained results, you can observe that as the heating temperature increases, the temperature difference between the sample surface and its core (1/2 of the length of the sample heating zone) increases.

The maximum value of the core sample temperature of 1469°C was achieved at the stage of heating sample to a temperature of 1435°C, which lead to local remelting of the sample and forming a zone being a mixture of the liquid and solid phases. TABLE 5 summarizes the computed and measured temperature differences between the sample core and its surface.

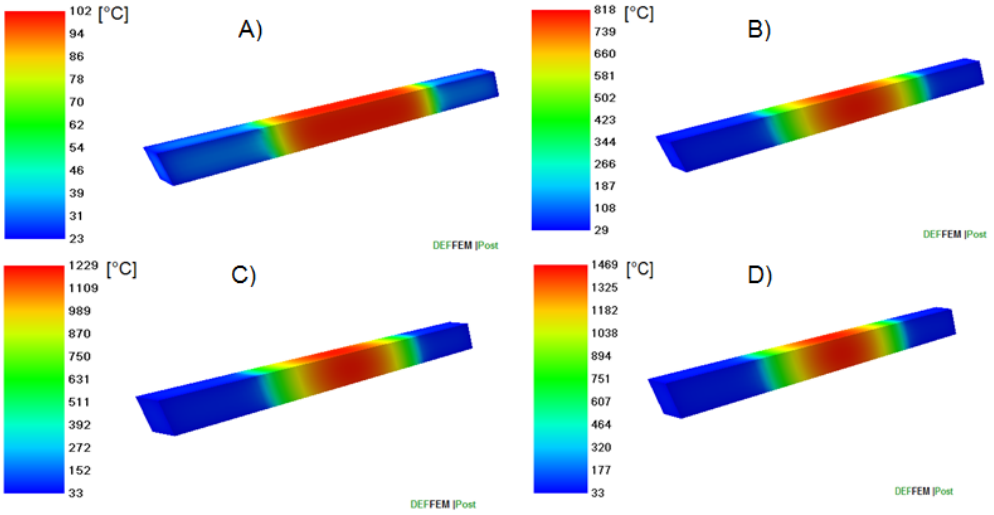

Fig. 2. The temperature field obtained as a result of resistance heating to a nominal temperature of A) 100°C, B) 800°C, C) 1200°C, D) 1435°C

TABLE 5

Summary of measured and computed temperature differences between the sample core and its surface

Experiment						
TC4, (°C)	100	300	500	800	1200	1435
TC3, (°C)	105.68	305.40	507.37	816.32	1226.22	1481.47
TC3-TC4, (°C)	**5.68**	**5.40**	**7.37**	**16.32**	**26.22**	**46.47**
Simulation						
NTC4, (°C)	100	300	500	800	1200	1435
NTC3, (°C)	102.99	304.64	511.98	818.19	1229.11	1469.18
NTC3-NTC4, (°C)	**2.99**	**4.64**	**11.98**	**18.19**	**29.11**	**34.18**

During the execution of experimental tests, metallographic specimens were made on selected longitudinal sections (the central part of a sample and the lengths 5 and 10 mm from the sample core) and cross-sections (core and the length of 10 mm from the sample core). Places of specimens selected this way enabled the obtained micro model results to be tentatively verified and qualitatively evaluated. In Fig. 3 an example macrostructure obtained by the experiment and their digital representation obtained by simulation are presented. The number of grains, average aspect ratio, and average circularity in the visible area are the primary morphometric parameters allowing for preliminary verification of the developed model of grain micro-growth.

The maximum value of relative error in presented example was: number of grains (9.65%), average aspect ratio (6.91%), and average circularity (20.17%). Morphometric analysis made in other sections of the sample was characterized by a relative error within 6-30%.

4.3. Modeling the shape of the deformation zone – example results

The simulations of high-temperature deformation were performed in accordance with the methodology of experimental

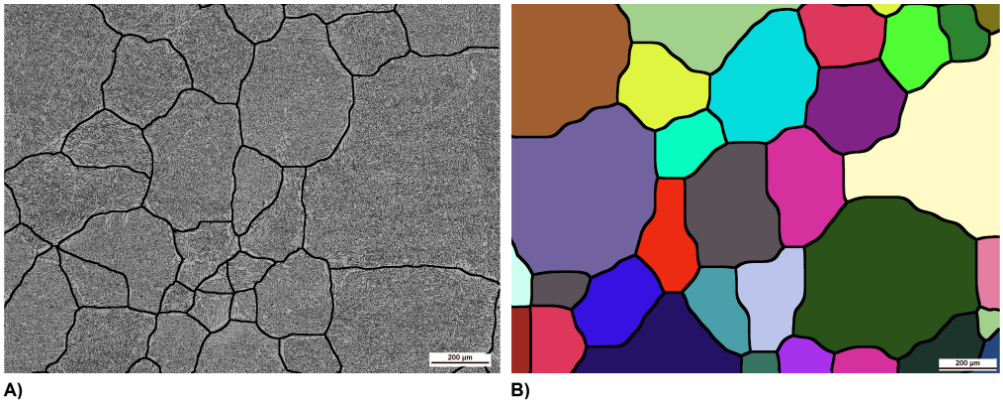

Fig. 3. Example macrostructure, A) experiment and B) digital representation (core of the sample, longitudinal section)

tests presented in section 2. Cuboidal samples with a length of 124 mm were subject to deformation assuming a stroke of 5 mm and a stroke rate of 1 mm/s. Fig. 4 present examples of results in the form of strain intensity fields, for test simulations of deformation at temperatures of 1200, 1350, 1400 and 1435°C. In all cases the maximum values of strain intensity are cumulated in the central part of the sample (deformation zone), however the nature of its distribution varies. For simulations in the temperature ranges 1200-1400°C (without the formed mixed phase in the sample core), the maximum values of strain are obtained on the whole sample cross-section (from the sample core to its surface), and their value increases as the nominal deformation temperature increases. For the test simulation of deformation at a temperature of 1435°C, a different nature of distribution can be observed. As a result of resistance heating to the nominal deformation temperature in the sample core a mushy zone formed, being a mix of the solid and liquid phases. The maximum sample core temperature was 1469°C (Fig. 2), and the liquid phase fraction estimated by the micro model was $f_l = 0.098$. In this case accumulation of the maximum strain values included primarily the area of the sample core (mushy zone).

In order to preliminarily verify the formulated mathematical model of steel deformation in the semi-solid state for predicting the size and shape of the deformation zone, the following verification criteria were assumed: a) the measurement of the length of the deformed zone, b) the measurement of the cross-section. A photogrammetric system by GOM Atos Triple Scan was used to digitize the actual samples to a binary form. Analyses and measurements of the deformation zone were made using firmware of GOM Inspect v7.5 scanner. The obtained measurements were averaged and summarized in TABLE 6.

Analyzing the obtained results, we could observe that as the temperature of the deformation test increased, the length of the deformation zone shortened, and the maximum transverse dimension of the deformation zone increased. The relative error was within 1.76-25.38% for the first criterion, whereas for the second criterion it was 6.68-16.77%. Simulations of deformation for temperatures above 1445°C with a reduction of 5 mm failed. The mushy zone present in the sample core, where the strain was the highest, at the same time was the area of a large deformation of the finite element mesh. Consequently, it leads to lack of convergence of optimization procedures and an interruption of computing.

TABLE 6

Summary of measurements of the deformed zone length and its cross-section (experiment vs. simulation)

	Deformed zone			Mean cross-section		
T (°C)	Exp. (mm)	Sim. (mm)	Relative error (%)	Exp. (mm)	Sim. (mm)	Relative error (%)
1200	31.11	37.15	**19.41**	12.11	11.30	**6.68**
1300	27.53	33.78	**22.70**	12.32	11.33	**8.03**
1350	26.39	33.09	**25.38**	12.66	11.37	**10.18**
1400	26.68	27.15	**1.76**	12.34	11.48	**6.97**
1435	14.57	17.02	**16.81**	14.61	12.16	**16.77**

5. Performance tests

The performance tests (grain-growth model) were conducted on a workstation equipped with the Intel Core i7 Extreme CPU, 24 GB of RAM and three NVIDIA GeFore GTX cards [17]. The main aim of the research was to determine the optimal CUDA parameters: $q_{k/MC}$ – number of kernel calls per step, MC, $q_{b/k}$ – number of blocks per kernel calls, $q_{th/b}$ – number of threads per block, $q_{c/th}$ – number of calculating cells per threads. The total computation times were analyzed for various CUDA parameters (τ_{total}). The following parameters of the micro model (see sub-chapter 3.3) were adopted for the results presented in the paper: exponent of mobility function $n = 3$, initial grain orientation number $Q_{grain} = 54$, one million cells per one finite

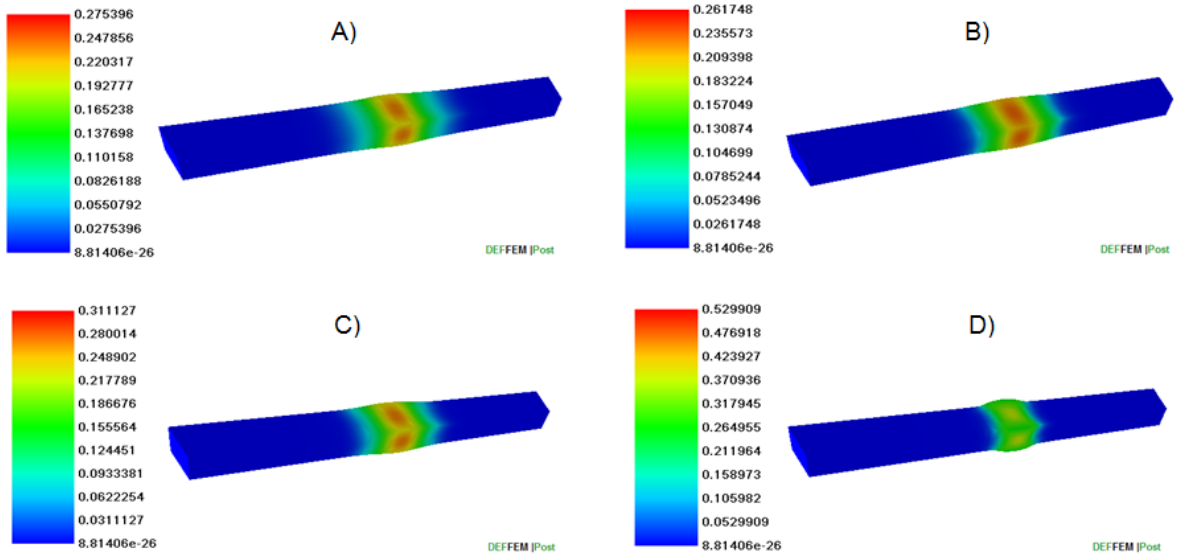

Fig. 4. Strain intensity field (test at a temperature of A) 1200°C, B) 1350°C, C) 1400°C, D) 1435°C)

element, 100 Monte Carlo steps per 10 seconds simulation time. In order to increase the efficiency of the algorithm, the following modifications were made:

– stopping calculations in areas where the probability of a cell state change is not greater than 0,
– including cells located on grain boundaries in calculations (cells inside the grain with the same neighbors are not included in the calculations).

The best identified parameters of CUDA are as follow: $q_{k/MC} = 1$, $q_{b/k} = 4883$, $q_{th/b} = 512$, $q_{c/th} = 1$. For the selected parameters of the grain growth model, the simulation time on GPU and single-threaded CPU was equal 19 and 1134 seconds, respectively.

6. Summary

This paper presents main assumptions of the hybrid model for high-temperature steel processing within temperature ranges close to the solidus line. The hybrid model of steel deformation in the conditions of two phase (liquid and solid) coexistence adapted to spatial states is an innovative solution. The presented mathematical model is original as it modifies the power functional of a classic rigid-plastic solution to include local density variations in the mathematical model at a level of mechanical solution. In order to generate a digital representation of macrostructure in the volume of the sample tested, the thermo-mechanical model can be optionally coupled with the grain micro growth model. GPU based on possibility of comprehensive simulation of grain growth in the resistance heating process combined with local remelting (taking into account the formation of the mushy zone) followed by free/controlled cooling of the sample tested is the original solution of the micro model. The following fundamental conclusions can be drawn from the completed work:

a) The accuracy of estimation of force parameters for a extra-high temperature tensile processes (DIM methodology) and compression processes (NIM methodology) is within relative error limits 3.4-9.1%. The exception was the test at a temperature of 1200°C, where the error was 28.5%.
b) As regards the simulation in the micro scale and generating a digital representation of the macrostructure, the morphometric analysis parameters were within the relative error limits of 6-30%.
c) The accuracies of estimation of the length of the deformed zone and the cross-section were within the error limits 1.76-25.38% and 6.68-16.77%, respectively.
d) The conducted model tests showed practical limitations in application of the formulated numerical models (the reduction of 5 mm and the maximum (nominal) deformation temperature of 1445°C).
e) GPU support was used in order to increase the computational efficiency of the grain growth model. There was a 59-fold increase in the computing speed on the GPU compared to single-threaded computing on the CPU.

Acknowledgment

The work was realized as a part of fundamental research financed by the Ministry of Science and Higher Education, grant no. 16.16.110.663.

REFERENCES

[1] G. Sa, I. Mihaiela, I. Roderick, L. Guthrie, Progress of strip casting technology for steel – historical developments, ISIJ Int. **52** (12), 2109-2122 (2012).
[2] M. Rosso, I. Peter, Continuous casting and rolling for the manufacturing of thin Al sheets, J. Ach. Mat. Manuf. Eng. **52** (2), 59-66 (2012).
[3] V. Kumar, Thermo-mechanical simulation using gleeble system-advantages and limitations, J. Met. Mat. Sci. **58** (1), 81-88 (2016).
[4] V. Kumar, C.S. Lin, J.A. Sekhar, Semi-solid deformation in multi-component nikel alumide, J. Mat. Sci. **28**, 3581-3588 (1993).
[5] C.S. Lin, J.A. Sekhar, Solidification morphology and semi-solid deformation in superalloy Rene 108-equiaxed solidified microstructures, J. Mat. Sci. **29**, 3637-3642 (1994).
[6] J.Y. Lin, S. Sugiyama, J. Yanagimoto, Microstructural evolution and flow stress of semi-solid type 304 stainless steel, J. Mat. Proc. Tech. **161** (3), 396-406 (2005).
[7] D.J. Seol, et al., Phase-field modelling of the thermo-mechanical properties of carbon steels, Acta Mat. **50** (9), 2259 2268 (2002).
[8] H. Shimahara, et al., Investigation of flow behaviour and microstructure on X210CrW12 steel in semi-solid state, Sol. St. Phen. **116-117**, 189-192 (2006).
[9] Z. Sun, et al., Numerical simulation of mechanical deformation of semi-solid material using a level-set based finite element method, Mod. Sim. Mat. Sci. Eng. **25** (6), 1-15 (2017).
[10] J. Fonseca, et al., In situ study of granular micromechanics in semi-solid carbon steels, Acta Mat. **61** (11), 4169-4179 (2013).
[11] A. Kalaki, M. Ketabchi, Predicting the rheological behavior of AISI D2 semi-solid steel by plastic instability approach, Am. J. Mat. Eng. Tech. **1** (3), 41-45 (2013).
[12] J. Ghorpade1, et al., GPU processing in CUDA architecture, Adv. Comp.: Int. J. **3** (1), 105-120 (2012).
[13] M. Głowacki, Modelowanie matematyczne i symulacje komputerowe odkształcania metali – teoria i praktyka, 2016 AGH Kraków.
[14] M. Hojny, Modeling steel deformation in the semi-solid state, 2018 Springer, Switzerland.
[15] M. Hojny, M. Głowacki, P. Bała, P. Bednarczyk, W. Zalecki, A multiscale model of heating- remelting-cooling in the Gleeble 3800 thermomechanical simulator system, Arch. Metall. Mater. **64** (1), 401-412 (2019).
[16] Q. An., et al., The bending, impact fracture behavior and characteristics of stainless steel clad plates with different rolling temperature, Arch. Metall. Mater. **66** (1), 229-239 (2021).
[17] T. Dębiński, M. Hojny, T.T.T. Nguyen, D. Cedzidło, Parallel numerical calculation on GPU for the 3-dimensional model of grain growth in steel samples subjected to heating-remelting-cooling process in the Gleeble 3800 thermo-mechanical simulator (not published), (2021).